CICE 2023 Rio de Janeiro – Brazil 11TH INTERNATIONAL CONFERENCE ON FRP COMPOSITES IN CIVIL ENGINEERING

Optimization of tensile properties and bond behaviour to concrete of fibre reinforcement strands produced within a dynamic fibre winding process

Tom Rothe, Technical University Braunschweig, Germany, t.rothe@tu-braunschweig.de
Julia Pösch, Technical University Braunschweig, Germany, julia.poesch@tu-braunschweig.de
Stefan Gantner, Technical University Braunschweig, Germany, stefan.gantner@tu-braunschweig.de
Norman Hack, Technical University Braunschweig, Germany, n.hack@tu-braunschweig.de
Christian Hühne, Technical University Braunschweig, Germany, christian.huehne@dlr.de

ABSTRACT
For the integration of reinforcement directly into additively manufactured structures a Dynamic Winding Machine (DWM) is developed, in which fibre material is consolidated to a strand and provided with a surface structuring. The produced reinforcement strands are formed into reinforcement structures with the help of an end effector attached to a robot. In combination with robotic integration strategies additively manufactured structures can be reinforced by this process. Results from mechanical, chemical and optical investigations presented in this paper aims to gain fundamental knowledge about the properties of the reinforcement strands produced by the newly developed process.

KEYWORDS
Additive Manufacturing in Construction; Pull-out Tests; Robotic Fibre Winding; FRP Concrete Reinforcement; Textile-Reinforced Concrete; Textile reinforcement production

INTRODUCTION
Integrating reinforcement into 3D-printed concrete components remains one of the biggest challenges for Additive Manufacturing with concrete (Buswell et al., 2020; Kloft, Empelmann, Hack, Herrmann & Lowke, 2020; Mechtcherine et al, 2021). Within the collaborative research centre TRR 277 “Additive manufacturing in construction” (AMC) the production of individualized structures by different 3D concrete printing processes (3DCP) is investigated (Kloft et al., 2021). In particular particle bed printing, extrusion and Shotcrete 3D printing (SC3DP) are focused. The integration of reinforcement is a major concern for the production of weight-bearing 3DCP components. Due to the layerwise production by 3DCP the integration of reinforcement needs to be rethought (Kloft et al., 2020). Especially the integration of reinforcement perpendicular to the printing layer is a great challenge. Within the research project A05 “Integration of Individualized Prefabricated Fibre Reinforcement in Additive Manufacturing with Concrete” a holistic process for the production of an individualised, in situ and robot-based fibre reinforcement is developed, realised and tested. Robotic integration strategies for fibre reinforcement were developed that are applicable to different 3DCP techniques (Gantner, Rothe, Hühne & Hack, 2022). In combination a fully automated process for additively manufactured reinforced concrete elements is possible. The goal is to establish a process for the automated and in situ production. Therefore, the process-parallel production of reinforcement structures has to be as compact and simple as possible. The complexity of the reinforcement production process is reduced to a minimum compared to classic pultrusion or winding processes. At the same time, the quality of the reinforcement strand should remain as high as possible. To fulfil these requirements a Dynamic Winding Machine (DWM) is developed, in which fibre material is consolidated to a strand and is provided with a surface structuring. An earlier version of the machine has been presented by Hack (Hack et al., 2021). The strands combine a fibre material, e. g. glass or carbon fibre, with an epoxy resin as matrix material. A secondary fibre material, e. g. different types of yarn or twisted yarn, is wound helically around the primary fibre strand. By varying different production perimeters and the used materials adapted reinforcement strands for the special needs of different 3DCP techniques and structural elements can be produced.

The DWM is designed to be integrated directly into a robot-based production process. The reinforcement strands are formable into individualized reinforcement structures with the help of an end effector attached to a robotic arm.
For a validation of the produced reinforcement strands different investigations are conducted. By mechanical testing as well as optical (laser scanning microscopy) and chemical investigation (thermogravimetric analysis (TGA)) a characterisation of the properties of the reinforcement strands is achieved. The aim is to gain fundamental knowledge about the properties of the reinforcement strands. Based on a first series of tension and pull-out testing a second series of pull-out testing is conducted to optimize bonding properties and to gain further knowledge on the influence of the adjustment of different parameters during production.

SAMPLE FABRICATION

A developed Dynamic Winding Machine (DWM) is used to manufacture reinforcement strands. The working principle is shown in Fig. 1. To produce reinforcement strands with a defined diameter the amount and size of primary fibre rovings are varied. The procedure presented in this paper focuses on glass fibre material as core fibre, referred to as primary fibre strand in the following. The DWM is also designed to process other fibre materials such as carbon fibres or basalt fibres. The primary fibre strand is impregnated with epoxy resin. A secondary fibre strand is wound around the primary fibre strand to create a surface profiling to increase the interlocking and bond between concrete and the reinforcement strand. The impregnation of the secondary fibre strand is conducted by excess resin from the impregnated primary fibre strand. The DWM allows for the variation of different geometrical properties of the produced reinforcement strands. In addition to varying the raw materials, it is possible to vary several parameters of the reinforcement strands, e. g. the winding density of the secondary fibre strand and, by means of a hysteresis brake, the pretension with which the secondary fibre strand is wound.

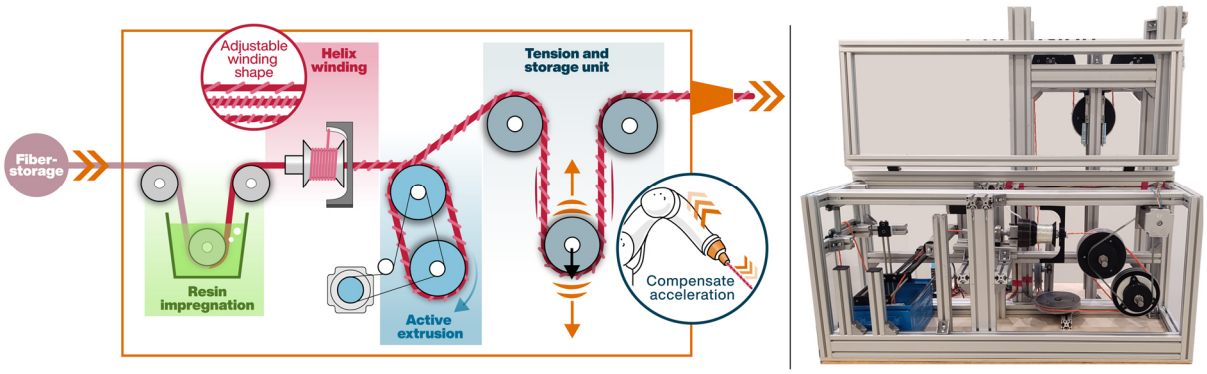

Figure 1: Schematic illustration of the fibre preparation process and the assembled Dynamic Winding Machine (DWM)

As described in the introduction, it is possible to freely shape the strands produced by the DWM using a robotic end effector (s. Fig. 2). However, for the mechanical characterisations aimed at here, straight bars are needed. To simplify the production, the reinforcement strand is pulled out of the DWM by hand and straight bars are produced via a pin grid. After curing, the bars are cut to the required length. For the purpose of simplicity, these will be referred to as DWM rebars in the following.
Various types of surface structuring by winding a secondary fibre have already been investigated in literature (Malvar, 1995; Solyom & Balázs, 2020). As the overall production process presented here differs significantly from classical production variants, it is necessary to quantify the rebars produced. The aim is to determine which machine settings have which influence on the mechanical properties. In the long term, the aim is to adapt the surface structuring of the DWM rebars for each 3DCP method in such a way that the best result is achieved in real applications. Among other things, the tensile and bonding behaviour to concrete must be weighed against each other. As reinforcement variations different secondary glass fibres types (roving, yarn and twisted yarn) and different secondary fibre strand winding densities are used. Another variant is to change the tension when winding the secondary fibre by altering the braking power of the hysteresis brake. Further adjustments to the

completed reinforcement strand are made after the strand leaves the DWM and are described in more detail below.

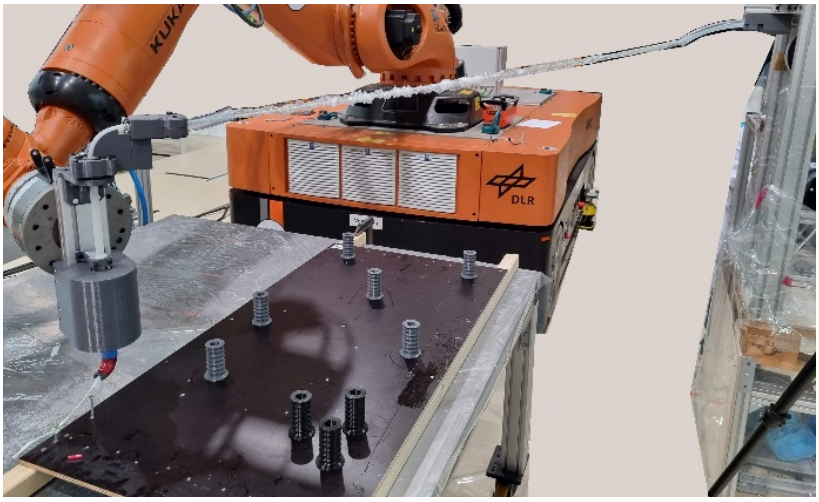

Figure 2: Robotic processing of reinforcement strands produced by the DWM

The nomenclature for different specimen in this paper is shown in Fig. 3. As reference the reinforcement type *D4-H300-T8* is used. It represents a DWM rebar with a diameter of 4 mm (further referred to as d_s), a hysteresis brake setting of 300 mA and twisted yarn as secondary fibre strand with a rib spacing of 8 mm. Used diameters in this paper are 4 mm (19200 tex of primary glass fibre), 6 mm (45300 tex) and 8 mm (76800 tex). The amount of primary fibre is calculated for a fibre volume content (FVC) of 60 %. As hysteresis brake setting 100 mA (approx. 17,5 Nmm of resistance) for small indentations and 300 mA (approx. 112 Nmm of resistance) for higher indentations of the primary fibre strand are used. As secondary fibre material a 410 tex glass fibre roving (ECR16 410 908, Chaghai Composite Materials), a 300 tex yarn (EC13 300 Z20, Culimeta) and a 3x136 tex twisted yarn (EC-9 136 X3 S135, Culimeta) is used. As a modification, excess resin on the surface is stripped off to determine whether a reduced outer epoxy resin layer has an effect on the bond strength. As another modification the reinforcement strands are additionally tensioned after winding on the pin grid by adding a weight force. Thus, shape deviations in the strands, which can occur due to winding on the pin grid and curing, are to be prevented. Additionally, two different commercially available rebars are tested, which are designated T-D*x*-A/B-*xx*. Series A has a similar structure as the DWM rebars. A thread is wound helically around the uncured primary fibre strand, which results in severe indentations and protrusions. Series B is manufactured using a classical pultrusion process. Subsequently, ribs are milled into the hardened bar. All sample series and the tests carried out on them are listed in Tab. 1. For modifications a reference sample series is used.

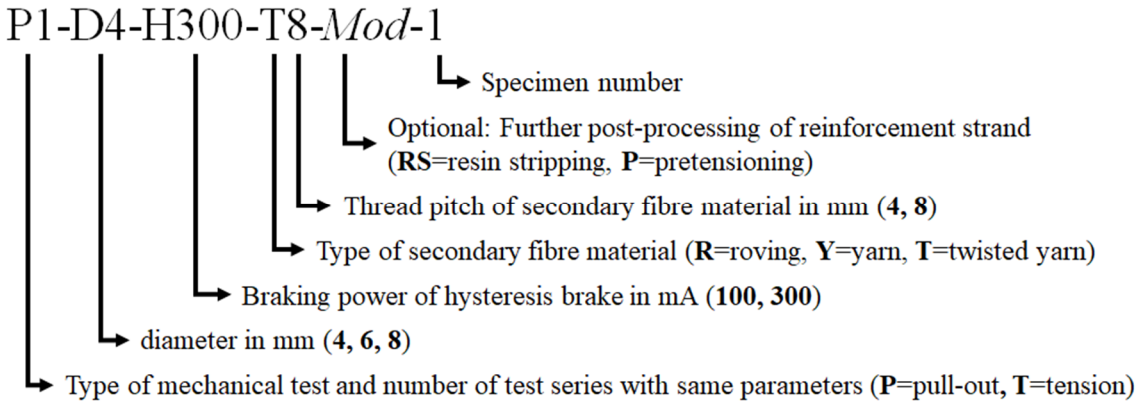

Figure 3: Specimen description with used parameters

Table 1: Investigated sample series in this paper

Sample series	Conducted investigations	Sample series	Conducted investigations
D4-H100-T8	T, P, optical	D4-A	T, P
D4-H300-T8 (reference)	T, P (twice), optical, TGA	D6-A	T, P
		D8-A	T, P
D6-H300-T8	T, P	D8-B	P
D8-H300-T8	T	D4-H300-T4	P
D4-H300-T8-RS	P, optical	D4-H300-Y8	P, optical
D4-H300-T8-P	P, optical	D4-H300-R8	P

Tensile specimens

Following ASTM D7205-21 (ASTM, 2021) each rebar is cut to the specified length. Both ends are anchored in steel sleeves. The length and diameter of the sleeve depends on the diameter of the rebar (s. Tab. 2). The anchor is attached to the rebar using the same epoxy resin the bar is made out of. An alignment plug is used to centre the FRP bar inside the sleeve. It is sealed using silicone. An external jig is built to ensure the alignment of the rebar relative to the sleeves. It is shown in Fig. 4.

Table 2: Size of tensile specimens

d_s [mm]	sleeve length [mm]	free length [mm]	sleeve diameter [mm]
4	200	380	20
6	250	380	21,3
8	350	380	25

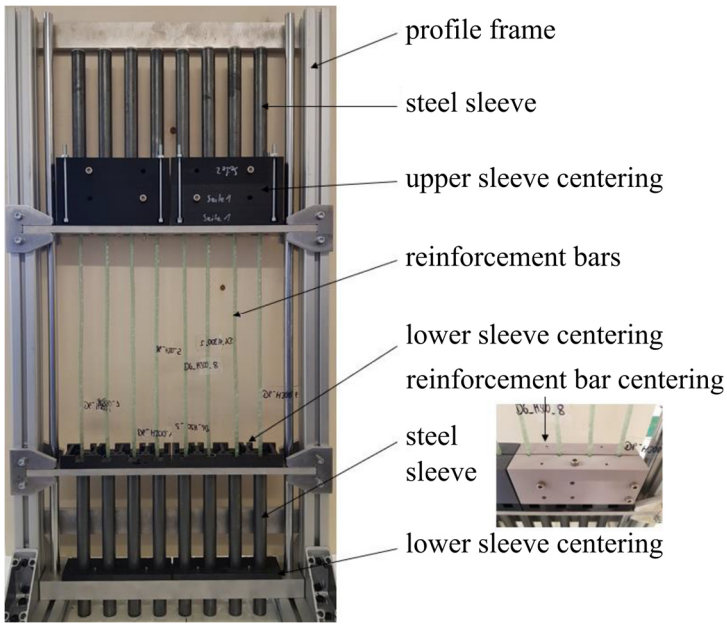

Figure 4: Centering jig for the production of tensile and pull-out specimens

Pull-out specimens

Following RILEM RC6 (RILEM TC, 1983) the rebars are cut to a length of 600 mm and are anchored in a steel sleeve at one side. The process is the same as explained for the tensile specimens. The other end is embedded in a concrete cube with an edge length of 200 mm. To ensure the dimensions of the concrete a wooden mould is used. The bond length (l_b) between concrete and rebar is equals five times the diameter of the rebar (d_s). To ensure the desired bonding length plastic tubes and plugs are used to keep the concrete away from the bonding area. The rebar is centred by the plug within the plastic tube and the mould. Each plug is produced by rapid prototyping and made to fit each rebar diameter. After assembling the mould and sealing it using silicone the plastic tubes, the plugs and the rebar are placed into the mould. A sprayable, fine-grained concrete (max. aggregate size = 2 mm) is used and mixed in a compulsory mixer like described by Freund (Freund & Lowke, 2022). The concrete is also used for

SC3DP within the research network TRR 277. In order to obtain the required amount of concrete for all samples, a total of four batches of concrete are mixed. After 3 min of mixing the fresh concrete is poured into the moulds. An additional compaction of the concrete is carried out. Afterwards the final specimens are cured for 28 days in a temperate room at 20°C and a relative humidity of 65%. To test the strength of the concrete three additional concrete cubes are produced for every batch.
Overall, two test series with 24 specimens each are conducted. After evaluating the results of the first test series, the sample series D4-H300-T8 is selected as reference. For the selection, it is taken into account that 4 mm reinforcement strands are stable to produce and the bond strength is slightly higher than for sample series D4-H100-T8. Based on it, production parameters for the DWM rebars of the second test series are varied.

TESTING

Tensile testing

The tensile properties are tested displacement-controlled following ASTM D7205-21 (ASTM, 2021) with a displacement rate of 4 mm/min. The rebar is mounted in a hydraulic testing machine (Zwick). A tensile force is applied and measured until the bar fails. A 300 mm extensometer is placed centrally within the free length of the rebar to determine its elongation. The force, the machine displacement and the elongation are recorded. As described in the introduction, the sample production is a newly developed process with reduced complexity. In order to be able to detect possible variations in the production process, 8 DWM rebars are tested for every sample series. As the commercial rebars are assumed to have a low scatter, 3 specimens of each sample series are tested.

Bond testing

The bonding properties are tested displacement-controlled following RILEM RC 6 (RILEM TC, 1983). To execute the pull-out test a hydraulic testing machine (Walter + Bai AG) is used. The concrete block is placed with the sleeve embedded end of the rebar pointing upwards. At the short end of the rebar the displacement is measured. The tensile force (F) is applied through the steel sleeve anchor at the upper end. A displacement rate of $v_p = 0.02$ mm/s is used. The setup for the pull-out test is shown in Fig. 5. For each sample series of DWM rebars 4 specimens are tested and for each sample series of commercial rebars 3 specimens are tested.

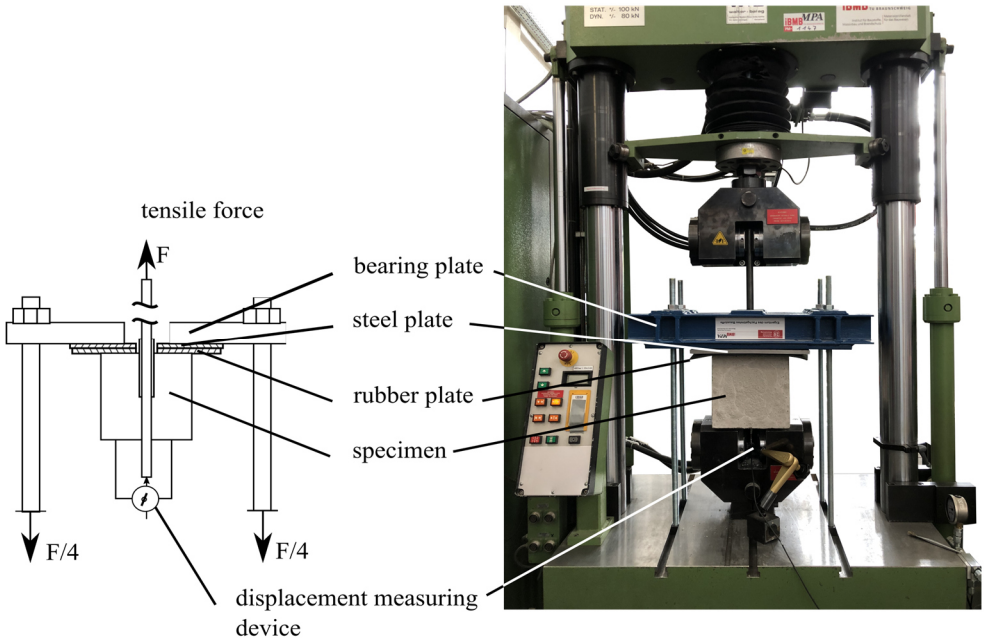

Figure 5: Test setup for pull-out testing according to RILEM RC 6 (RILEM TC, 1983)

Determination of the fibre volume content and fibre distribution
The fibre volume content (FVC) is exemplary determined from the DWM rebar P1-D4-H300-T8-5 (reference sample series), which is not tested mechanically. 5 specimens of 150-170 mg each are sawn out of the rebar every 20 cm. Every specimen is subjected a thermogravimetric analysis (TGA) by the procedure described in DIN 16459 (DIN, 2021) to determine its FVC (TGA/DSC 3+ from METTLER TOLEDO). To gain information on the distribution and undulation of the fibre filaments inside the DWM rebars two transverse sections and two longitudinal sections of some sample series are examined with a laser scanning microscope.

RESULTS AND DISCUSSION

Mechanical testing
The Young's modulus and the tensile strength is calculated based on ASTM D7205-21 (ASTM, 2021) and the results obtained are compared with ASTM D7957-22 (ASTM, 2022). The results are shown in Fig. 6. It is shown that the Young's modulus of the self-made sample series is lower than the modulus of the tested, commercial rebars. It decreases slightly from 4 to 8 mm bar diameter. It ranges between 33.5 GPa and 40.8 GPa. According to ASTM D7957-22 (ASTM, 2022), the required minimum Young's modulus of 44,8 GPa for glass fibre reinforced rebars is not achieved. The Young's modulus of the commercial rebars is nearly constant with increasing diameter and increases from 47.2 GPa till 49.7 GPa. The decrease with increasing diameter in the DWM rebars can be explained by increased production-related inaccuracies of the reinforcement strands. This also explains the increasing scatter. The scatter is significantly greater than that of the commercial rebars, which show hardly any scatter. It is noticeable, that the reference sample series (P1-D4-H300-T8) has a lower Young's modulus than the sample series P1-D4-H100-T8. Both series differ only in the hysteresis brake setting and thus in the indentation of the secondary fibre strand. These stronger indentations lead to increased undulation of the primary fibre strand and, in conjunction with the resulting reduced minimum bar diameter, are held responsible for the decrease. This additionally leads to an increased scattering. A more detailed evaluation of the undulation is given below.
For tensile strength, the results are partly different. The tensile strength of the DWM rebars decreases from 851 MPA (P1-D4-H100-T8) to 649 MPA (T1-D8-H300-T8), while the tensile strength of the commercial rebars increases from 613 MPa (4 mm) to 793 MPa (8 mm). Based on these results, only P1-D4-H100-T8 meets the requirement of ASTM D7957-22 (ASTM, 2022). The decrease in the DWM rebars can be attributed to the same effects identified for Young's modulus. The increase for the commercial rebars could be related to a reduced undulation due to smaller indentations in relation to the rebar diameter.

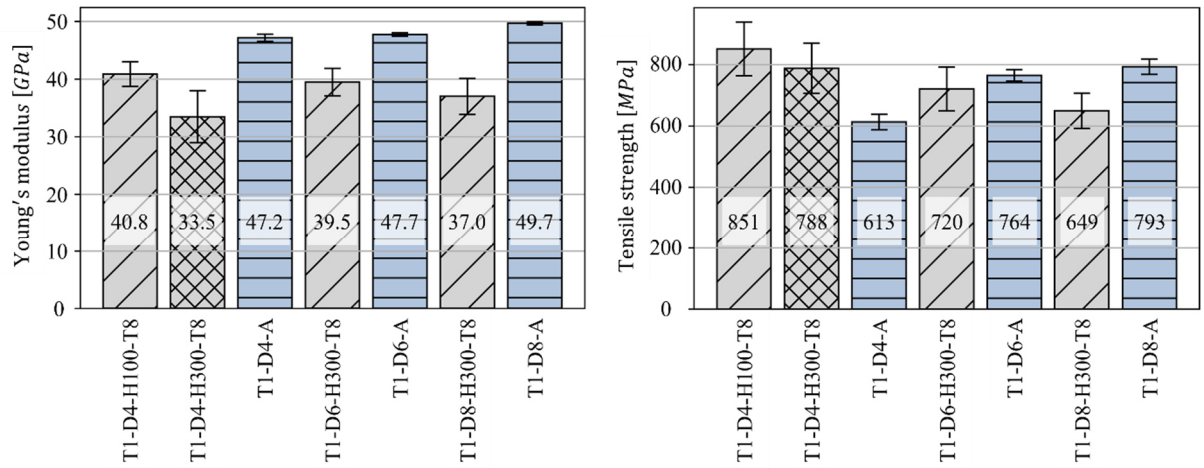

Figure 6: Young's modulus and tensile strength from tensile testing (reference with cross pattern)

The bond strength is calculated by the maximum force divided by the bond area (s. Eq. 1). The results are shown in Fig. 7.

$$\tau = \frac{F}{\pi \cdot d_s \cdot l_b} \qquad \text{Eq. 1}$$

For the comparison of the individual test series, the different concrete strengths of the concrete batches used must be taken into account. An assignment of the sample series to the corresponding batches is shown in Tab. 3. The batches of the second test series have an overall higher concrete strength, which, according to literature, also causes increased bond strength (Shunmuga Vembu & Ammasi, 2023). Since the reference sample series is tested in both test series, it is used to evaluate the adaptations made in the sample series.

Table 3: Concrete strength of different batches

Concrete batch	Concrete strength [N/mm²]	Pull-out sample series
1	59.3	P1-D4/6/8-A, P1-D8-B
2	56.3	P1-D4-H100-T8, P1-D4-H300-T8, P1-D6-H300-T8
3	65.0	P1-D4-H300-T8-P, P1-D4-H300-T4, P1-D4-H300-Y8
4	62.7	P2-D4-H300-T8, P1-D4-H300-T8-RS, P1-D4-H300-R8

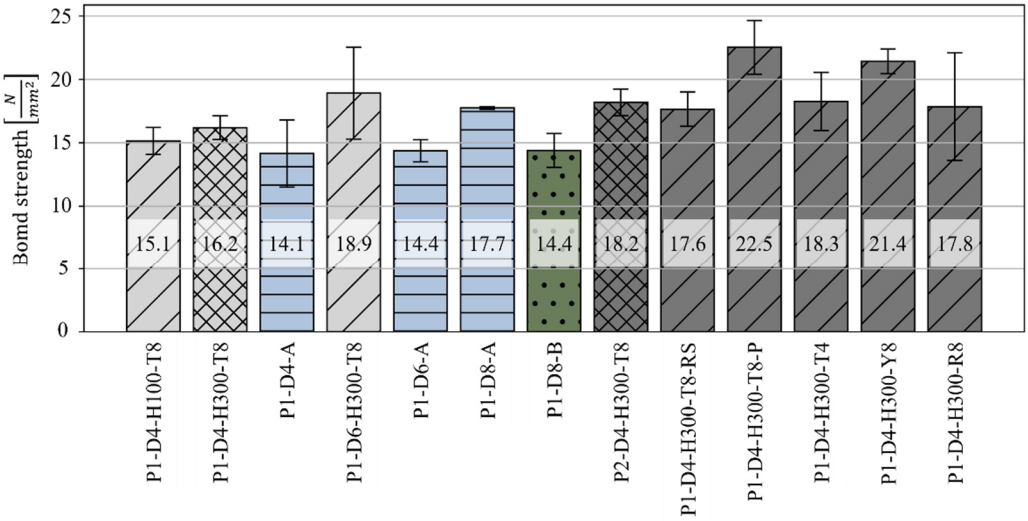

Figure 7: Bond strength from pull-out testing with sample series from second test series in dark grey

To determine the maximum force for the bond strength calculation the information of force over time (s. Fig. 8) and force over slip (s. Fig. 9) is used. The slip on the free end of the rebar is measured by a displacement measuring device. Due to the test setup the slip can only be measured till a maximum pull-out distance of 4 mm.
By evaluating the shown plots in Fig. 8 and Fig. 9 for all specimens different types of failure can be determined. In specimen P1-D4-H300-T8-1 and -3, an abrupt drop in force occurs when the maximum force is reached. Afterwards, the force increases again, but remains clearly below the maximum force. This is due to mechanical interlocking between the rebar and the surrounding concrete. This interlocking is suddenly loosened by shearing off the concrete bracket or shearing off e.g. a bulge in the rebar. Afterwards the rebar continues to move through the concrete with reduced force. For P1-D4-H300-T8-1 a maximum is reached, which steadily decreases and settles at a lower force level till it further decreases. Mechanical interlocking also occurs here, whereby this does not decrease abruptly due to a failure of the components, but the bar forces itself through the concrete and either the concrete or the bar surface is continuously scraped off. The failure mode for nearly all DWM sample series and the commercial sample series P1-A-4/6/8 is a pull-out of the rebar out of the concrete without a splitting of the concrete or a rupture of the DWM rebar. Rupture occurs only for three specimens (P1-A-4-3, P1-A-6-3, P1-D4-H300-R8-1).

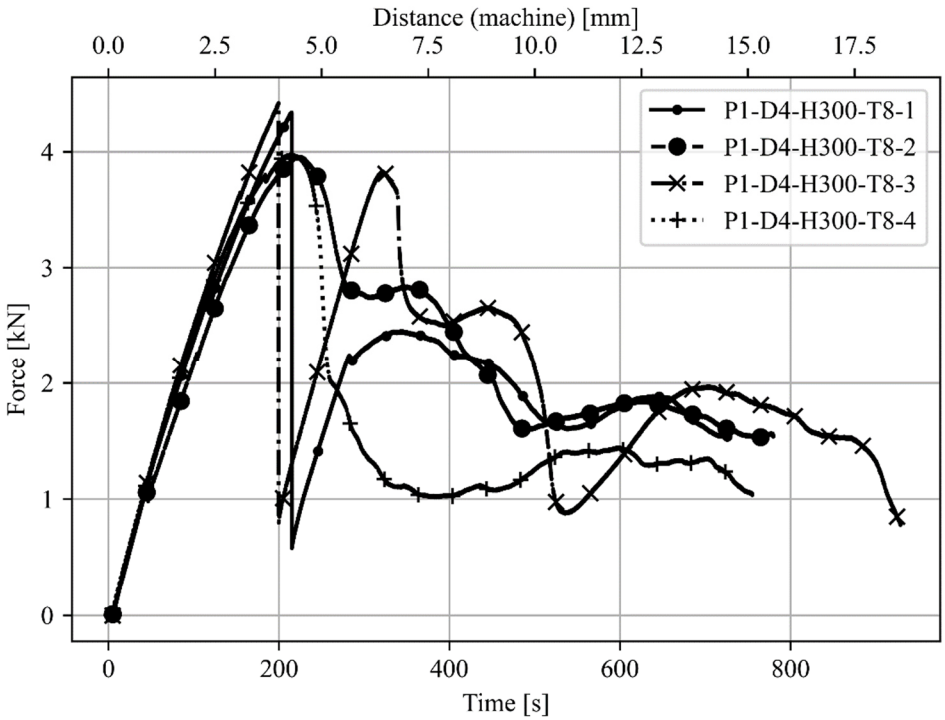

Figure 8: Force during pull-out testing plotted over time exemplary for sample series P1-D4-H300-T8

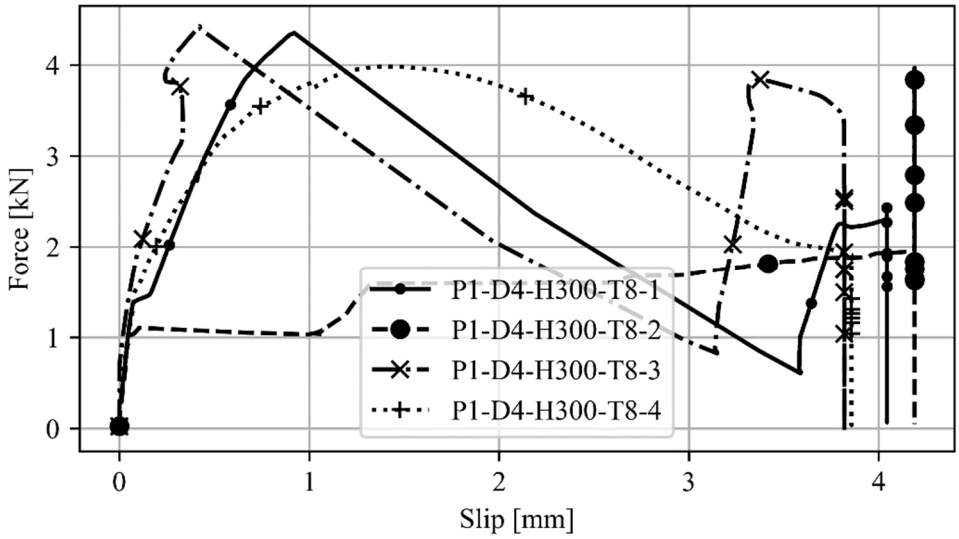

Figure 9: Force during pull-out testing plotted over slip exemplary for sample series P1-D4-H300-T8 (marking every 8 s)

Tested specimen from different sample series are shown in Fig. 10. The most common case of failure is shearing of the protruding areas between the indentations by the secondary fibre strand. Based on the results from Fig. 7 it can be determined, that all tested specimen, commercial and DWM rebars, have a bond strength in the same order of magnitude. If the different concrete strengths are taken into account by a correction factor and the mean value of all bond strengths is calculated, more than 90% of all specimens lie in the interval of +/- 2-times the standard deviation.

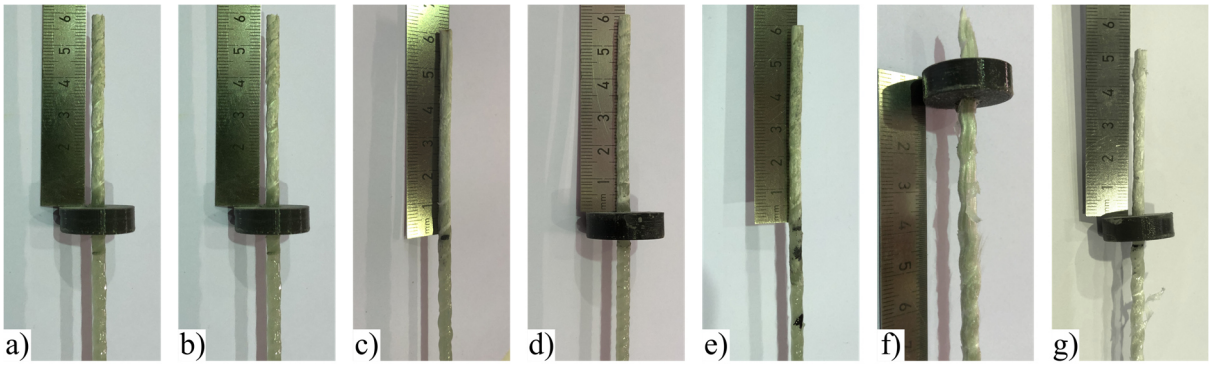

Figure 10: Damage patterns of different specimen of the pull-out testing: **a)** P2-D4-H300-T8-1, **b)** P1-D4-H300-T8-RS-4, **c)** P1-D4-H300-T8-P-3, **d)** P1-D4-H300-T4-1, **e)** P1-D4-H300-Y8-1, **f)** P1-D4-H300-R8-1, **g)** P1-D4-H300-R8-3

Fibre volume content analysis

The FVC for the tested reference sample series specimen (P1-D4-H300-T8-5) is 62,66% with a standard deviation of only 0,61% and a void content of 1,96%. The fibre mass content is 79,21% and fulfils the requirement of ASTM D7957-22 (ASTM, 2022). The FVC is very close to the desired and calculated FVC of 60%. Nevertheless, one need to consider that the fibre filaments are not equally distributed about the cross section, which can be seen in Fig. 11 a). In the area of the applied secondary fibre strand the filaments are well compacted (s. Fig. 11 c)). At the opposite part of the cross section the filaments are less compacted (s. Fig. 11 b)). Additionally, excess resin can be found at the surface of the strand, especially in the area of the applied secondary fibre strand (upper left part of Fig. 11 a)). The Figures 11 a-c) show, that the FVC is not constant across the cross section. This implies, that the nominal FVC in the inner and mechanically bearing part of the reinforcement strand is higher than the determined 62,66%. The void content of 1,96% is mainly bundled in the excess resin at the strand surface. Furthermore, foreign particle inclusions can be detected. Besides smaller voids Fig. 11 d) shows the inclusion of a foreign particle. While cleaning the surface the foreign material is smudged across the surface (right part of Fig. 11 d)). In Fig. 11 e) the connection area of the secondary fibre strand, here a twisted yarn, and the primary fibre strand is shown. It is noticeable, that the impregnation with epoxy resin just through excess resin of the primary fibre strand is sufficient.

Besides the transverse section of the reinforcement strand the longitudinal section is investigated by laser scanning, too. Two exemplary longitudinal sections are shown in Fig. 12. The specimen P1-D4-H300-T8 (Fig. 12 a)) is grinded down till the centre of the rebar. The specimen P1-D4-H300-T8 is grinded down less than 1 mm from its outer surface. Fig. 12 a) shows the inner distribution of the primary fibre strand. As presumed, undulation results from the indentations of the secondary fibre strand. However, the broken and partly torn out fibre strands in the longitudinal direction of the bar show that the undulation is within a manageable range. Fig. 12 b) shows a longitudinal section of the rebar close it its outer surface. There are many pores detectable in the left area of Fig. 12 b). Like assumed by the results of the TGA for the reference sample series pores form primarily in the outer layer of excess resin. In addition, on the right end of Fig. 12 b) one can see how the two rovings, which form the primary fibre strand, are twisting into each other. This is due to the current production setup within the DWM. The aim should be to redesign production so that the primary fibre strands are as straight and untwisted as possible.

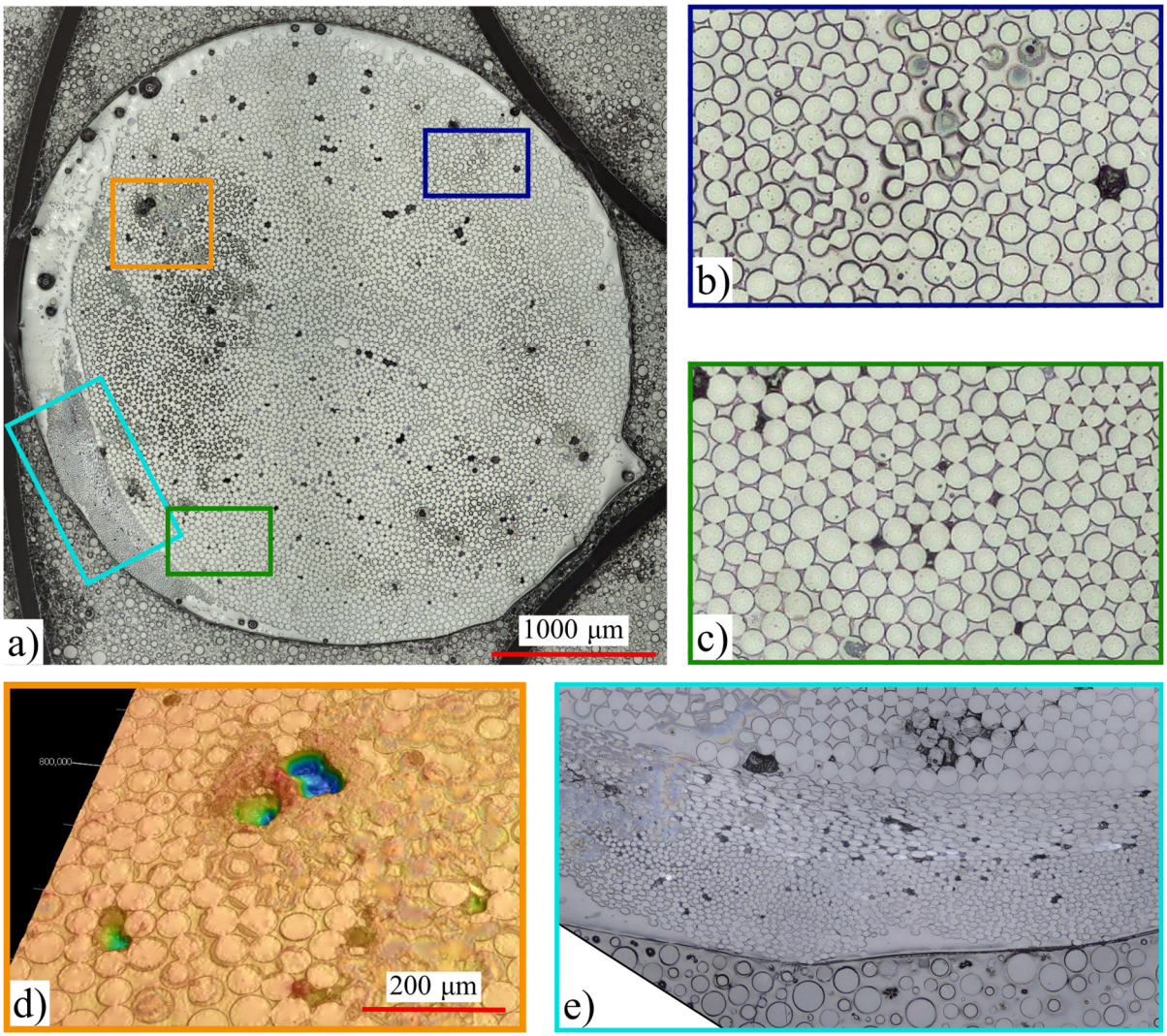

Figure 11: Investigation of transverse sections of P1-D4-H300-T8: **a)** complete cross section, **b)** close up opposite to secondary fibre strand, **c)** close up next to secondary fibre strand, **d)** 3D-image of void and foreign particle inclusion, **e)** close up of secondary fibre strand

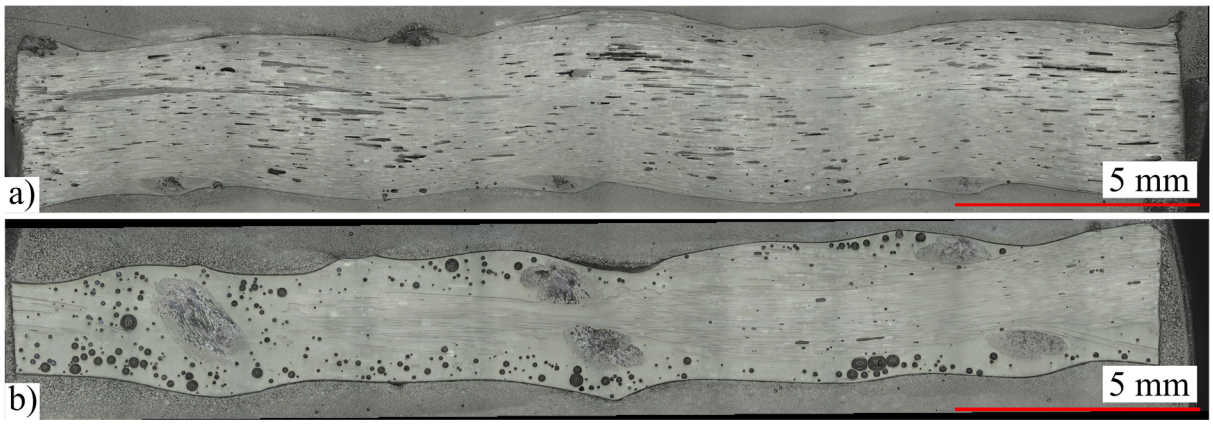

Figure 12: Investigation of longitudinal sections of P1-D4-H300-T8 (a) and P1-D4-H100-T8 (b)

CONCLUSION

In this paper an approach is presented to produce individualized reinforcement structures for a robot-based process directly on the construction site. In combination with concrete 3D-printing, novel and freely formable structures can be produced. The production of the reinforcement strands is done with a specially developed Dynamic Winding Machine (DWM). Reinforcement strands from glass fibre

and epoxy resin are produced with different production parameters and are mechanically tested. From the results shown, the following statements can be derived:

- It is shown that the mechanical properties of DWM rebars are in the range of commercial fibre rebars. While the bond strength is even a little higher, the tensile properties are mostly slightly lower than those of commercial rebars. The requirements given by ASTM D7957-22 (ASTM, 2022) are not yet reached.
- Increasing the bar diameter leads to increased scatter in the production process. This also increases the scattering in the mechanical properties. To reduce this, the production quality must be further increased with the DWM.
- Due to the high scatter, the close proximity of the results and the small number of specimens, especially for the bond testing, only a low statistical certainty can be assumed for the results obtained here. Further tests with an increased number of specimens would be necessary to increase this certainty.
- The use of twisted yarn or yarn gives similarly results. Roving as secondary fibre material leads to high scattering and should therefore not be used. Increased indentation due to a stronger hysteresis brake setting has hardly any influence on the bonding behaviour, but reduces the Young's modulus and the tensile strength.
- Pre-stressing the reinforcement strands leads to significantly improved bond behaviour. It can be assumed that the tensile properties are also improved. This should be investigated further. In general, it can be deduced from this that a focus should be placed on the prestressing of the fibre strands in robotic fabrication. The aim should be to quantify the pretension in order to be able to draw a precise conclusion about optimal pretension. Stripping off excess resin has no significant influence on the bonding behaviour.
- The FVC is as desired and the resin impregnation across the reinforcement strand is very good. Still, the FVC reached by classical pultrusion processes is higher. To increase the FVC, the resin impregnation and compaction of the reinforcement strands must be optimised.
- The secondary fibre materials are sufficiently impregnated with resin. The more tightly the secondary fibre is wound, the more the primary fibre strand undulates. In addition, the primary fibre is twisted in itself as a result of the production process. This should be reduced in the future by adjusting the DWM.

CITATIONS

ASTM. (2021) Standard Test Method for Tensile Properties of Fiber Reinforced Polymer Matrix Composite Bars (ASTM D7205/D7205M − 21). West Conshohocken, PA. ASTM International.

ASTM. (2022) Standard Specification for Solid Round Glass Fiber Reinforced Polymer Bars for Concrete Reinforcement1 (ASTM D7957/D7957M − 22). West Conshohocken, PA. ASTM International.

Backes, J. G., Del Rosario, P., Luthin, A., & Traverso, M. (2022). Comparative Life Cycle Assessment of End-of-Life Scenarios of Carbon-Reinforced Concrete: A Case Study. Applied Sciences, 12(18), 9255. https://doi.org/10.3390/app12189255

Buswell, R. A., Da Silva, W. L., Bos, F., Schipper, H. R., Lowke, D., Hack, N., Kloft, H., Mechtcherine, V., Wangler, T., & Roussel, N. (2020). A process classification framework for defining and describing Digital Fabrication with Concrete. Cement and Concrete Research, 134, 106068. https://doi.org/10.1016/j.cemconres.2020.106068

Cadenazzi, T., Dotelli, G., Rossini, M., Nolan, S., & Nanni, A. (2020). Cost and environmental analyses of reinforcement alternatives for a concrete bridge. Structure and Infrastructure Engineering, 16(4), 787–802. https://doi.org/10.1080/15732479.2019.1662066

DIN. (2021) Bestimmung des Faservolumengehaltes (FVG) von faserverstärkten Kunststoffen mittels Thermogravimetrischer Analyse (TGA) (DIN 16459). Berlin. Beuth Verlag GmbH.

Freund, N., & Lowke, D. (2022). Interlayer Reinforcement in Shotcrete-3D-Printing. Open Conference Proceedings, 1, 83–95. https://doi.org/10.52825/ocp.v1i.72

Gantner, S., Rothe, T.-N., Hühne, C., & Hack, N. (2022). Reinforcement Strategies for Additive Manufacturing in Construction Based on Dynamic Fibre Winding: Concepts and Initial Case Studies. Open Conference Proceedings, 1, 45–59. https://doi.org/10.52825/ocp.v1i.78

Hack, N., Bahar, M., Hühne, C., Lopez, W., Gantner, S., Khader, N., & Rothe, T. (2021). Development of a Robot-Based Multi-Directional Dynamic Fiber Winding Process for Additive Manufacturing Using Shotcrete 3D Printing. Fibers, 9(6), 39. https://doi.org/10.3390/fib9060039

Kloft, H., Empelmann, M., Hack, N., Herrmann, E., & Lowke, D. (2020). Reinforcement strategies for 3D-concrete-printing. Civil Engineering Design, 2(4), 131–139. https://doi.org/10.1002/cend.202000022

Kloft, H., Gehlen, C., Dörfler, K., Hack, N., Henke, K., Lowke, D., Mainka, J., & Raatz, A. (2021). TRR 277: Additive manufacturing in construction. Civil Engineering Design, 3(4), 113–122. https://doi.org/10.1002/cend.202100026

Malvar, L. (1995). Tensile and Bond Properties of GFRP Reinforcing Bars. ACI Materials Journal, 92(3). https://doi.org/10.14359/1120

Mechtcherine, V., Buswell, R., Kloft, H., Bos, F. P., Hack, N., Wolfs, R., Sanjayan, J., Nematollahi, B., Ivaniuk, E., & Neef, T. (2021). Integrating reinforcement in digital fabrication with concrete: A review and classification framework. Cement and Concrete Composites, 119, 103964. https://doi.org/10.1016/j.cemconcomp.2021.103964

RILEM TC. (1983) Bond test for reinforcement steel. 2. Pull-out test (RILEM RC 6). E & FN SPON.

Shunmuga Vembu, P. R., & Ammasi, A. K. (2023). A Comprehensive Review on the Factors Affecting Bond Strength in Concrete. Buildings, 13(3), 577. https://doi.org/10.3390/buildings13030577

Solyom, S., & Balázs, G. L. (2020). Bond of FRP bars with different surface characteristics. Construction and Building Materials, 264, 119839. https://doi.org/10.1016/j.conbuildmat.2020.119839

ACKNOWLEDGEMENT

Funded by the Deutsche Forschungsgemeinschaft (DFG, German Research Foundation) – TRR 277/1 2020 – Project number 414265976. The authors thank the DFG for the support within the CRC/ Transregio 277 - Additive Manufacturing Construction. (Project A05).

CONFLICT OF INTEREST

The authors declare that they have no conflicts of interest associated with the work presented in this paper.

DATA AVAILABILITY

Data on which this paper is based is available from the authors upon reasonable request.